

Article

Potential and Scale-Up of Pore-Through-Flow Membrane Reactors for the Production of Prebiotic Galacto-Oligosaccharides with Immobilized β -Galactosidase

Ines Pottratz ^{1,*} , Ines Müller ¹ and Christof Hamel ^{1,2}

¹ Applied Biosciences and Process Engineering, Anhalt University of Applied Sciences, Bernburger Str. 55, 06366 Koethen, Germany; ines.mueller@hs-anhalt.de (I.M.); christof.hamel@hs-anhalt.de (C.H.)

² Institute of Process Engineering, Otto von Guericke University, Universitaetsplatz 2, 39109 Magdeburg, Germany

* Correspondence: ines.pottratz@hs-anhalt.de; Tel.: +49-3496672522

Abstract: The production of prebiotics like galacto-oligosaccharides (GOS) on industrial scale is becoming more important due to increased demand. GOS are synthesized in batch reactors from bovine lactose using the cost intensive enzyme β -galactosidase (β -gal). Thus, the development of sustainable and more efficient production strategies, like enzyme immobilization in membrane reactors are a promising option. Activated methacrylatic monoliths were characterized as support for covalent immobilized β -gal to produce GOS. The macroporous monoliths act as immobilized pore-through-flow membrane reactors (PTFR) and reduce the influence of mass-transfer limitations by a dominating convective pore flow. Monolithic designs in the form of disks (0.34 mL) and for scale-up cylindrical columns (1, 8 and 80 mL) in three different reactor operation configurations (semi-continuous, continuous and continuous with recirculation) were studied experimentally and compared to the free enzyme system. Kinetic data, immobilization efficiency, space-time-yield and long-term stability were determined for the immobilized enzyme. Furthermore, simulation studies were conducted to identify optimal operation conditions for further scale-up. Thus, the GOS yield could be increased by up to 60% in the immobilized PTFRs in semi-continuous operation compared to the free enzyme system. The enzyme activity and long-time stability was studied for more than nine months of intensive use.

Keywords: pore-through-flow membrane reactor; enzyme immobilization; β -galactosidase; galacto-oligosaccharides; simulation studies; operation modes



Citation: Pottratz, I.; Müller, I.; Hamel, C. Potential and Scale-Up of Pore-Through-Flow Membrane Reactors for the Production of Prebiotic Galacto-Oligosaccharides with Immobilized β -Galactosidase. *Catalysts* **2022**, *12*, 7. <https://doi.org/10.3390/catal12010007>

Academic Editors: Maria Elena Russo and Giuseppe Olivieri

Received: 2 December 2021

Accepted: 20 December 2021

Published: 22 December 2021

Publisher's Note: MDPI stays neutral with regard to jurisdictional claims in published maps and institutional affiliations.



Copyright: © 2021 by the authors. Licensee MDPI, Basel, Switzerland. This article is an open access article distributed under the terms and conditions of the Creative Commons Attribution (CC BY) license (<https://creativecommons.org/licenses/by/4.0/>).

1. Introduction

Functional foods with positive effects on health are becoming increasingly important [1]. One of the most common food additives used for functional food are prebiotics, which are substrates that are selectively utilized by host microorganism conferring a health benefit [2]. They serve as “feed” for the intestinal bacteria and thus influence the growth and activity of a healthy intestinal microbiota [3]. A greater interest exists in utilization of galacto-oligosaccharides (GOS) as health-promoting food supplement for infant as well as for clinical but also for animal nutrition [4]. Oligosaccharides can be found in nature, e.g., as part of human breast milk in high concentrations. In contrast, bovine milk contains oligosaccharides as minor components only [5,6]. Thus, a promising approach for GOS formation is provided by the enzymatic synthesis from bovine lactose using β -galactosidase (β -gal). Furthermore, as lactose is a side product of the dairy industry on a large scale, the enzymatic conversion to the prebiotic GOS offers a sustainable and value-added utilization of the resource.

The enzyme β -galactosidase (EC 3.2.1.23) performs two main reaction steps as shown in Figure 1. The first reaction step is the hydrolysis of lactose forming an enzyme-galactose-complex. Subsequently, a transgalactosylation reaction takes place when sugar acts as

galactosyl acceptor. The output is GOS whose structure differs by the regiochemistry of the glycosidic linkages and varying chain lengths, expressed by the degree of polymerization (DP). Typically, GOS consist of 1 to 5 galactose monomers with optional one glucose monomer at the end [7].

Otherwise, when water is the reaction partner of the enzyme-galactose-complex the hydrolysis reaction will be completed under galactose cleavage. The hydrolysis and transgalactosylation reaction proceed simultaneously and are limited by chemical equilibrium, resulting in a product mixture containing GOS, unreacted lactose, galactose and glucose [8]. Among them, the ratio of transgalactosylation and hydrolysis activity is strongly influenced by the choice of enzyme origin, referring to reviews by Torres et al. [8] and Fischer et al. [9].

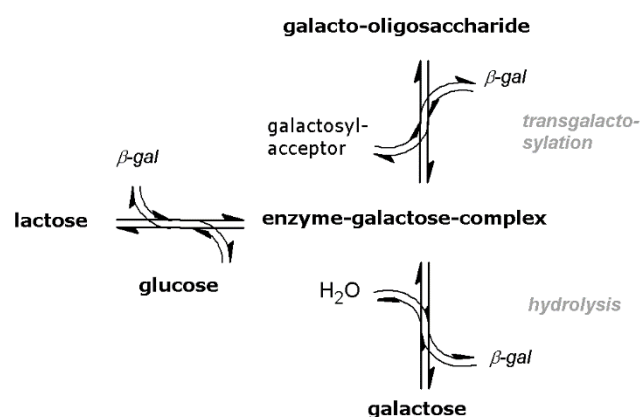


Figure 1. Equilibrium-limited reaction mechanism of enzymatic GOS synthesis with β -galactosidase [10].

However, the costs of a single use of β -gal for GOS synthesis in large-scale discontinuous batch processes are very high and limiting the industrial application. Thus, the immobilization of enzymes enables an improved sustainability of the process due to higher stability and recyclability of the enzyme and is widely used in bio-catalyzed processes. Reported immobilization of β -gal with focus on GOS synthesis can be classified according to the type of support, type of process and reactor design (continuous or batch) and the type of immobilization method, such as cross-linking, entrapped and covalent binding of the enzyme to the carrier. Wherein the enzyme immobilization via covalent binding generates strong and stable linkages and prevents leakage from the matrix [11].

As carrier for β -gal immobilization for GOS synthesis numerous materials are described in the literature and are reviewed by Ureta et al. [12]. Some materials with a focus on immobilization of β -gal from *B. circulans* are nanofibers [13,14] which are the most recently used application studies. A more widespread application to synthesize GOS in batch processes is the immobilization of β -gal on beads, such as Sepabeads® [15], Eupergit® [16,17], Purolite® [18] and others. Chitosan beads were used as support material for immobilization of β -gal from *B. circulans* [19] as well as from *K. lactis* [20] in batch processes or packed-bed reactors, both revealing a shift in the pH and temperature optima of the enzymes compared to a free enzyme system. Warmerdam et al. [17] immobilized β -gal from *B. circulans* on Eupergit® beads in a packed bed reactor. The immobilized enzyme showed a slightly higher hydrolysis activity and a lower GOS productivity than the free enzyme, which is probably the result of diffusion limitations in the microporous structure of the support. The utilization of microporous agarose beads with different modifications as immobilization support for β -gal from *B. circulans* did not lead to higher enzyme productivity or GOS yield [21].

While the influence of enzyme immobilization on reaction kinetics is inconsistently described in the literature, the studies reveal a significant impact of the carrier matrix and/or pore size for the enzyme activity with respect to GOS formation and a decisive role for mass transport limitations through diffusion in the micro pore structure itself. To overcome the diffusion limitation, which is associated with supports based on microporous particles,

carriers such as monoliths have been employed. One type of promising monoliths are convective interaction medias (CIM[®]) based on methacrylate polymer [22,23]. Methacrylate-based macroporous monoliths have suitable hydrodynamic properties, characterized by high mass flow and a high chemical and mechanical stability [23,24]. Furthermore, the monolithic supports allow a dominating convective transport of the target molecules into the pore structure to interact with the immobilized enzyme [25,26]. To realize a covalent linkage between enzymes and the methacrylate monolith the surface is activated with various functional groups, which directly influence the enzyme activity [25], the selectivity [27–29] and the steric hindrance based on immobilized enzyme mobility [30] (due to different lengths of the activation groups).

CIM[®], as an immobilization carrier, is mainly used as pore-through-flow membrane reactors (PTFR) and their main reported application area is proteomic analysis by immobilization of trypsin [30–33].

In the current state, the application of methacrylate based macroporous monoliths as immobilization carrier for GOS synthesis continuously operated PTFR is not reported by other research groups. Therefore, the characterization of the carrier in respect to the influence of the chemical activation to the enzyme properties, enzyme activity and transgalactosylation rate in the PTFR is crucial. In our previous work [34] β -gal from *B. circulans* immobilized on aldehyde, ethylendiamin and carbonyldiimidazole (CDI) activated monolithic PTFRs in the form of small scale disks have been studied and compared. The experiments demonstrated that a shift towards the transgalactosylation rate takes place compared to the free enzyme system in a batch reactor is possible. The best results regarding the maximum GOS yield and enzyme stability over 80 days were achieved with the CDI activated monolithic disk. Based on these results, enzyme immobilization with CDI was selected for the present study also taking into account the less complex chemistry as it requires fewer steps and chemicals [35].

In the present study, a scale-up of the immobilization of β -gal from *B. circulans* on 1 mL, 8 mL and 80 mL-PTFRs (cylindric small columns) with a CDI activation was performed using an initial lactose concentration of 100 g L⁻¹ (ILC). The results will be compared with the free enzyme system. The properties of immobilized enzyme were determined by the mass of bound enzyme, enzyme activity and kinetic parameters. The results regarding transgalactosylation activity were characterized and compared by GOS yield, the turnover-number (k_{cat}) and the space-time-yield (STY) for the free and immobilized systems. In order to increase the GOS yield, continuous and the semi-continuous operation modes were studied by various experiments. Working with additional recirculation opens up a further degree of freedom for reaction and process control to reuse the enzyme in multiple process cycles. To evaluate the potential and for further scale-up strategies first simulation studies in a pore-through-flow membrane reactor were carried out [10].

2. Results and Discussion

2.1. Evaluation of Immobilized Enzyme PTFRs and Kinetic Modeling

β -gal from *B. circulans* was covalent immobilized on carbonylimidazole activated methacrylate-based monoliths with different sizes and different flow profiles (see Section 3.3, Figure 8). The disk-PTFR has a total volume of 0.34 mL and the cylindric PTFRs have a total volume of 1, 8 and 80 mL. At an estimated porosity of 0.3, confirmed by determination of retention time by HPLC, the liquid volumes are as listed in Table 1 and represent the reactor volume in which GOS synthesis occurs.

Table 1. Disk/Reactor volumes for the free enzyme system (batch reactor) and the monolithic immobilized PTFRs as well as the mass and density of enzyme in the reactor systems.

Enzyme Reactor	V_{tot} [mL]	V_{liqu}^1 [mL]	m_{enz}^2 [mg]	$m_{\text{enz}} \text{ per } V_{\text{tot}}$ [mg mL ⁻¹]
batch reactor	40	40	9.02 ± 1.35	0.23
disk-PTFR	0.34	0.1	3.4 ± 0.24	10
1 mL-PTFR	1	0.3	8.4 ± 0.28	8.4
8 mL-PTFR	8	2.4	70.6 ± 0.10	8.8
80 mL-PTFR	80	24	439 ± 2.20	5.5

¹ liquid volume is calculated with a porosity of 0.3 for the PTFRs; ² determined with Biuret based reaction (\pm mean value deviations from duplicate determinations).

As expected, increasing the reactor volume leads to an increase in the mass of bound enzymes. The density in mg bound enzyme per mL monolith ranges from 5.5 for the 80 mL-PTFR to 10 for the disk (Table 1). The results indicate that similar specific amounts of enzyme were immobilized on the PTFRs whereby the 80 mL-PTFR represents an exception with its low enzyme density. The comparison of the immobilized PTFRs to the batch system with free enzyme is nevertheless evident, since significantly more enzyme mass per reactor volume is present in the PTFRs.

To study the kinetics of immobilized β -gal regarding the lactose conversion, the PTFRs in semi-continuous configuration were compared with the free enzyme in discontinuous batch reactors in (Table 2). K_M and V_{max} were estimated using Michaelis-Menten kinetics and Lineweaver-Burk linearization (Section 3.5.3). The comparison of K_M and k_{cat} between the immobilized and free β -gal is important, since it provides information on how immobilization influenced enzyme kinetics [25].

Table 2. Kinetic parameters, activities, enzyme-substrate-ratio (E/S), turn-over-number (k_{cat}) and space-time-yield STY of free and on PTFR immobilized enzyme, determined with semi-continuous configuration (Figure 2b).

Enzyme Reactor	K_M^1 [mmol L ⁻¹]	V_{max}^2 [mmol (L min) ⁻¹]	Activity ³ [U]	E/S ⁴ [U mg ⁻¹]	k_{cat}^5 [s ⁻¹]	STY ⁶ [g (L h) ⁻¹]
batch reactor	422 ± 14.5	13 ± 0.8	520 ± 31.0	120 ± 7.8	220 ± 14.3	17 ± 0
disk-PTFR	679 ± 10.0	173 ± 7.8	17 ± 1.4	1730 ± 25.0	19 ± 1.0	263 ± 50
1 mL-PTFR	602 ± 1.1	263 ± 11.9	79 ± 8.0	2630 ± 15.3	39 ± 2.5	260 ± 8
8 mL-PTFR	690 ± 8.0	217 ± 12.0	521 ± 11.4	2170 ± 9.0	30 ± 3.8	315 ± 26
80 mL-PTFR	614 ± 3.8	165 ± 8.2	3960 ± 15.9	1650 ± 25.0	23 ± 3.7	204 ± 18

¹ and ² are calculated for the lactose conversion; ³ one unit (U) is the conversion of one μmol lactose per min; ⁴ E/S = enzyme substrate ratio; ⁵ k_{cat} calculated from V_{max} and the approximate amount of β -gal (248 kDa); ⁶ STY in g GOS per hour and liter (liquid reactor volume), (\pm mean value deviations from duplicate determinations).

K_M values for immobilized β -gal on all four monoliths are similar: 602 mmol L⁻¹ (disk) to 679 mmol L⁻¹ (1 mL-PTFR). K_M for the free enzyme amounts 422 mmol L⁻¹. The affinity of the enzyme for its substrate lactose is therefore only slightly lower compared to the free enzyme system. In contrast, k_{cat} for the immobilized enzyme was significantly lower on all four scale-ups (19 to 39 s⁻¹) than for the free enzyme with 238 s⁻¹. For enzymes immobilized on methacrylate monoliths over covalent bonding, a slight increase in K_M and a decrease in k_{cat} commonly occurs [23,25,36]. The increase in K_M contributes to diffusion limitation but that is brought to a minimum using monolithic supports for immobilization [23,25]. On the other hand, k_{cat} is about 10 times lower for the immobilized enzyme than for the free one, which can be explained by a lower conversion rate of enzyme-substrate-complex into product [19]. Accordingly, it results in a reduced specific activity of the immobilized enzyme compared to the free enzyme. The specific activity is also lower for the immobilized β -gal than for the free enzyme with 58 U per mg free enzyme. It is 5 U mg_{enz}⁻¹ for the disk-PTFR, 9 U mg_{enz}⁻¹ for the 1 mL- and 80 mL-PTFR and 7 U per mg immobilized β -gal for the 8 mL-PTFR. This has already been described in the literature

and is described as a result of conformational and steric effects which occur during the covalent binding of the enzyme to the carrier surface [23,37,38].

Nevertheless, Table 2 also provides that the enzyme/substrate ratio (E/S) is much higher for immobilized enzyme in the reaction volume of the monoliths, such as in the discontinuous batch system. Thus, the STY and V_{max} , i.e., lactose hydrolysis, are higher than for the free enzyme. STY varies between 204 g (L h)^{-1} for the 80 mL-PTFR and $315 \text{ g GOS (L h)}^{-1}$ for the 8 mL-PTFR. Similar values of STY were described by Rodriguez-Colinas et al. [39], who immobilized β -gal from *B. circulans* on agarose beads in packed bed reactors with continuous configuration (ILC = 100 g L^{-1}).

In comparison of the values for the enzyme loading, as well as the kinetic parameters and activities, the scale-up of the immobilization can be considered successful, since the parameter values are similar, e.g., loading density or enzyme affinity (K_M). A difference in immobilization can be seen in the values by the disk. Although the loading density is the highest with 10 mg mL^{-1} support, the activity and the k_{cat} of the bound enzymes is the lowest. On the 80 mL monolith, the smallest amount of enzyme was bound per mL carrier. The activity, STY and k_{cat} are also the lowest here. The 1 mL- and 8 mL-PTFR provided the highest values.

2.2. Configuration Systems for GOS Synthesis in PTFR

Four reactor configurations with increasing complexity, as illustrated in Figure 2, were evaluated by experimental and model-based studies. The reference system is the discontinuous batch reactor with free enzyme (Figure 2a), whereas (b–d) are the reactor systems for immobilized enzymes striving for achieving intensified continuous process conditions.

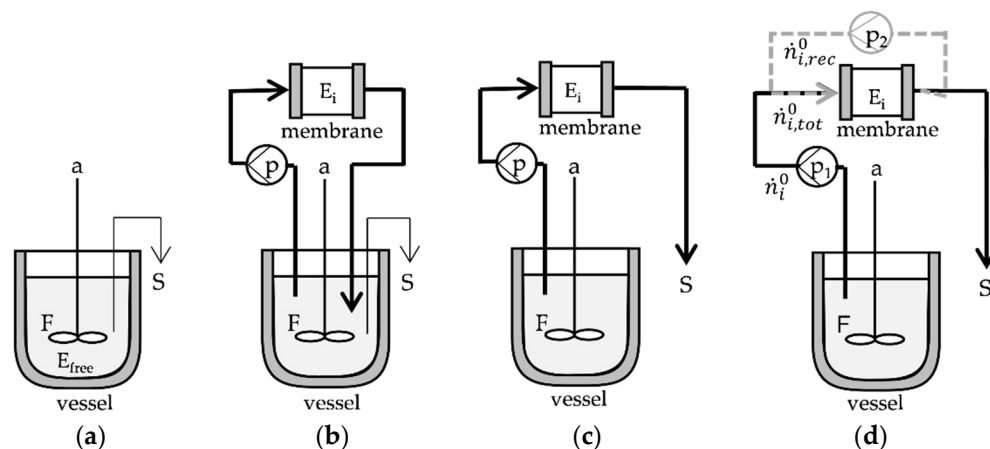


Figure 2. Reactor configurations for GOS synthesis: (a) discontinuous (batch) reactor with free enzyme (E_{free}) and (b) semi-continuous, (c) continuous (d) continuous with recirculation with immobilized (E_i) enzyme on monolithic PTFR (disk or 1 mL, 8 mL, 80 mL); F: feed stock solution (lactose), a: agitation, S: sampling, p: pump, n: amount of substance.

2.2.1. Continuous and Semi-Continuous Configuration

The synthesis of GOS with immobilized enzymes on monoliths was first investigated the continuous and semi-continuous operation for all PTFR sizes (Figure 2b,c). In the continuous process, with the feed only being passed through the monolith once, the enzyme catalyzed reactions are severely limited by the residence time, as the volume flow cannot be reduced infinitely. In the semi-continuous configuration, the substrate is circulated for a certain time, i.e., not converted lactose and GOS of different lengths come into contact with the enzyme several times. Thus, GOS with the desired higher DP and in higher yield can be synthesized.

For continuous configuration (Figure 2c) the experimental data for the scale-up from disk size up to 80 mL-PTFR is shown in Figure 3, wherein (a) represents the GOS yield as a

function of the flow rate and (b) as function of the residence time. The substrate lactose only passes through the monolith once. The GOS yield and the lactose conversion are therefore directly dependent on the residence time. The lower the flow, the higher the yield or conversion in the mass transfer limiting area [23,40]. The maximum achievable flows are 5 mL min^{-1} for the disk, 16 mL min^{-1} for the 1 mL-PTFR, 100 mL min^{-1} for the 8 mL-PTFR and for the 80 mL-PTFR 400 mL min^{-1} [35]. Limitations with regard to the enzyme catalyzed reaction in the PTFR are excessive low flow rates, which can lead to backmixing due to diffusion (see disk-PTFR: 0.05 mL min^{-1} in Figure 3a), and excessive high flow rates, which reduce the residence time too much.

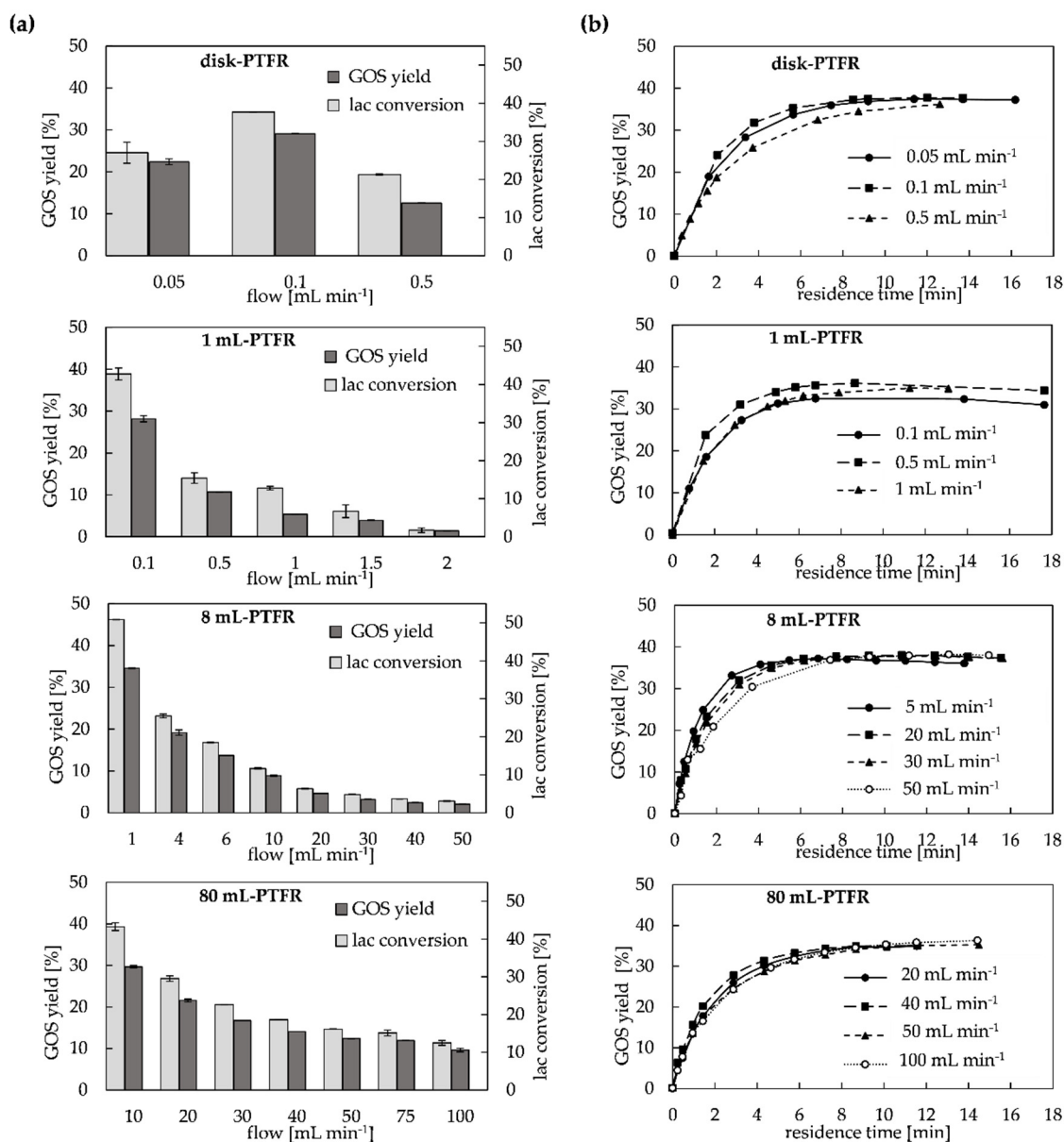


Figure 3. Performance of monolithic PTFRs (disk, 1 mL, 8 mL and 80 mL): (a) GOS yield and lactose conversion for the continuous configuration depending on the flow (ILC = 100 g L^{-1}); (b): GOS yield based on residence time (ILC = 100 g L^{-1}).

It is also demonstrated that an increase in the size of the monolith and the associated increase in the absolute amount of bound enzyme results in an increased product yield and conversion rate at the same flow rate. As shown in Figure 3a, a tenfold increase in the flow rate reduces the GOS yield by factor 3.5 for the 1 mL-PTFR and the 8 mL-PTFR

and by factor 2.7 for the 80 mL-PTFR. Despite minor differences in enzyme activity, the results show that the PTFRs can be easily scaled-up with regard to the transgalactosylation reaction in the continuous system. The exception here is once again the simple disk, which was limited in its application with regard to the volume flows, as back-mixing phenomena and an increase in pressure (above a maximum pressure of 18 bar) could be observed (Figure 3a). Although the methacrylate-based CIM[®] monoliths work without pressure loss, enhanced substrate concentrations (100 to 220 g L⁻¹ lactose) can lead to an increase in pressure [27]. Furthermore, the different flow rates also play a role here. The disk has an axial flow rate, whereas the cylindrical monoliths have a linear flow rate [35], as shown in Figure 8.

The studied semi-continuous configuration (Figure 2b) allows the substrate and already formed product to pass through the PTFR in several cycles. As described by [23,30], the flow rate in continuous systems has a marginal influence on the catalytic activity of the enzyme in GOS synthesis. Moreover, monolithic columns are not affected by diffusion limitations, hence residence time calculations become redundant when scaling up [35]. As shown in Figure 3b, the maximum average GOS yield of 37% (*w/v*) for an ILC of 100 g L⁻¹ was achieved at similar retention times (9 to 12 min) for all PTFRs. Nonetheless, the highest productivity with regard to the GOS synthesis can be observed for the 1 mL and 8 mL monoliths (Figure 3b), which is also reflected in the highest STY and E/S ratio (Table 2). A slightly reduced GOS yield (36%) is achieved with the immobilized enzyme in the 80 mL-PTFR, which was to be expected due to the lowest loading density, lowest E/S ratio (Table 2) and the more complex structure of the monolithic support for homogeneous flow distribution.

In Figure 4 the GOS yield of all four immobilized PTFRs with semi-continuous configuration is compared to the discontinuous batch system with free enzyme. The flow rates were 0.5 mL min⁻¹ for the disk- and 1 mL-PTFR, 10 mL min⁻¹ for the 8 mL-PTFR and 20 mL min⁻¹ for the 80 mL-PTFR. The GOS yield in the immobilized PTFRs reached about 37% and could thus be increased significantly compared to a yield of 23% GOS with the free enzyme system. The comparison of GOS yield vs. lactose conversion obtained with free or immobilized enzyme offered that the reaction has been shifted towards the transgalactosylation due to the increased E/S ratio in the reactor volume and the lack of diffusion limitation in the monolithic immobilized PTFRs (Figure 4b). The higher affinity of the immobilized enzyme towards the desired GOS synthesis than to hydrolysis is comparable with results obtained in [18,34]. The GOS degradation starts at a lactose conversion of 40% with the free enzyme and at a conversion rate of about 57% for the immobilized PTFRs (Figure 4b), which leads to the synthesis of GOS with a higher, favorable degree of polymerization. Similar observations were described for the immobilization of β -gal from *A. oryzae* on gelatin nanofibers [13], which achieved a GOS yield that was 10% higher than obtained with the free enzyme (ILC = 400 g L⁻¹). Another study with differently modified agarose showed that immobilization has a more critical impact on the lactose hydrolysis than on the transgalactosylation reaction [36]. However, the immobilization of β -gal with focus on the enzyme origin *B. circulans* revealed contradictory results, depending on carrier material and process configuration. Immobilization on Eupergit[®] C250 L beads in continuous packed bed reactors was described with a six times higher GOS productivity than with free enzyme (ILC = 380 g L⁻¹) [17]. Urrutia et al. [21] received similar GOS yield and profiles for immobilized β -gal from *B. circulans* on agarose beads in repeated batch processes and the free enzyme. In this study, an ILC of 100 g L⁻¹ leads to an 60% increase in GOS yield for immobilized monolithic PTFRs compared to free enzyme in discontinuous batch configuration.

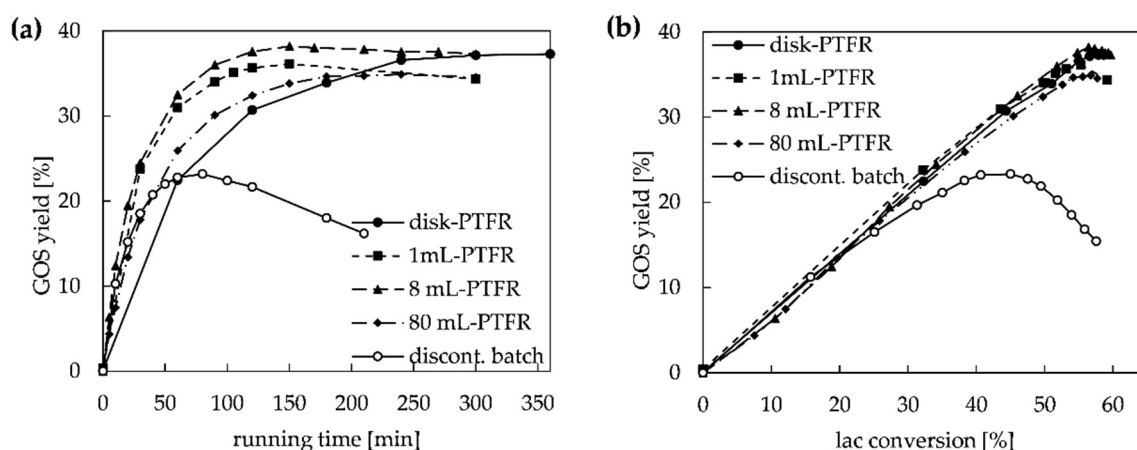


Figure 4. Comparison of the GOS yield obtained with the free enzyme in a discontinuous batch reactor and the immobilized enzyme with semi-continuous configuration in PTFRs, flow for disk and 1 mL-PTFR was 0.5 mL min^{-1} , for 8 mL-PTFR 10 mL min^{-1} and for 80 mL-PTFR 20 mL min^{-1} (ILC = 100 g L^{-1}): (a) GOS yield vs. experimental running time; (b) GOS yield compared to lactose conversion.

2.2.2. Continuous Configuration with Recirculation

The recirculation mode as third configuration for GOS synthesis in the immobilized PTFR was realized with the combination of semi-continuous and continuous configuration (Figure 2d). The addition of a recirculation step in the PTFR introduces a new degree of freedom for reaction and process control by allowing the enzyme to be reused in multiple process cycles. By adjusting the recirculation ratio to zero, it approaches more and more the continuous mode. In practical implementation, part of the volume flow after the monolith is returned to the inlet of the PTFR to convert the remaining lactose or to extend GOS chains. The recirculation volume ratio is controlled by pump 2, which obtains a significantly higher flow rate than provided by pump 1 (p1) for the feed flow. Thus, the flow rate through the PTFR results from the sum of flow rates of both pumps.

Initial tests were carried out with 100 g L^{-1} lactose in the 1 mL-PTFR, whereby the ratio of p1 to p2 and the flow through the monolith were varied to determine ideal classifications with regard to the preferred transgalactosylation reaction (Table 3).

Table 3. Flow settings for the recirculation system (Figure 2d) for GOS synthesis with immobilized β -gal on the 1 mL-PTFR (p = pump).

Recirculation Ratio	Flow Rate [mL min^{-1}]			Max. GOS Yield [%]
	p1 (Feed)	p2 (Recirculation)	Through PTFR	
1:10	0.09	0.91	1.00	20.27
1:10	0.06	0.60	0.66	25.55
1:5	0.17	0.83	1.00	15.01
1:5	0.10	0.50	0.60	21.00
1:2	0.33	0.67	1.00	10.44
1:2	0.10	0.20	0.30	22.23

The highest GOS yield with 25.55% was obtained with a high recirculation rate with a p1:p2 ratio of 1:10 while maintaining a small flow rate through the monolith with 0.66 mL min^{-1} (Table 3). The experiments with the lowest flow rate (0.3 mL min^{-1}) through the 1 mL-PTFR and the lowest recirculation ratio at the same time, however, deliver the second highest GOS yield with 22.23%. This indicates that the residence time of the substrate in the monolith obtains greater impact in the continuous configuration with recirculation than the recirculation rate. Furthermore, with increasing recirculation the feed concentration is

reduced by back mixing of the reactants with products. Thus, the reaction rate decreases as well as conversion. Nevertheless, the product can be removed continuously.

The experimental observations with respect to flow ratio with the 1 mL-PTFR were then transferred to the scale of 8 mL- and 80 mL-PTFRs. The recirculation ratios of 1:19 ($p_1 = 10.5 \text{ mL min}^{-1}$, $p_2 = 9.5 \text{ mL min}^{-1}$), 1:10 ($p_1 = 0.9 \text{ mL min}^{-1}$, $p_2 = 9.0 \text{ mL min}^{-1}$) and 1:5 ($p_1 = 1.7 \text{ mL min}^{-1}$, $p_2 = 8.3 \text{ mL min}^{-1}$) were studied experimentally with regard to the maximum GOS yield. The flow through the 8 mL- and 80 mL-PTFRs was 10 mL min^{-1} in each case, i.e., the retention time per flow ratio is the same for each monolith. Again, the highest GOS yield was determined with the highest ratio between feed flow and recirculation flow, which is 26% for both PTFRs (Figure 5). With a five-fold higher recirculation flow compared to the feed flow, the 8 mL-PTFR achieved a GOS yield of 17% and 22% with the 80 mL-PTFR (Figure 5a). However, the consideration of productivity of the continuous configuration with recirculation is important for scaling-up and evaluating the overall process. Thereupon it becomes apparent that the production of GOS in g per hour increases, although the maximum GOS yield is lower (Figure 5a). This is due to the fact that the feed flow (same as the product flow) with a setting of 1:19 is too slow to gain a correspondingly high amount of GOS.

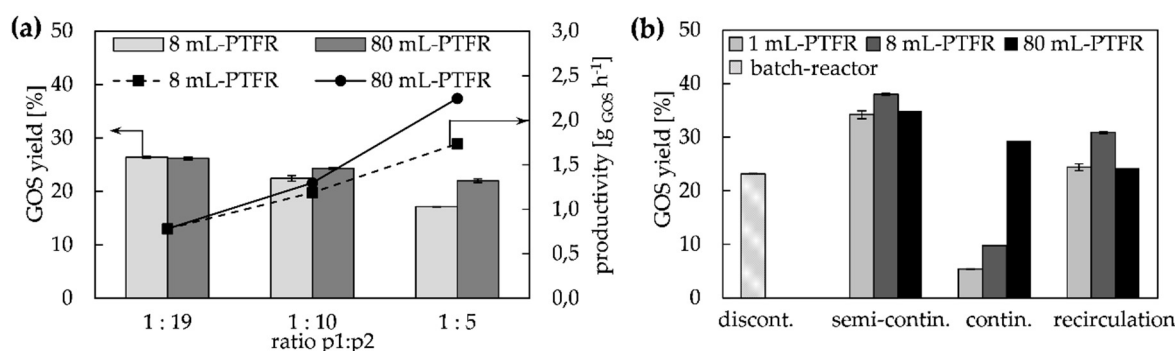


Figure 5. (a) GOS yield with immobilized β -gal on 8 mL- and 80 mL-PTFR with the recirculation system (Figure 2d), the rates describe the relationship between the feed flow rate (p_1) and the recirculation flow rate (p_2), the resulting flow rate through PTFRs was 10 mL min^{-1} ; (b) comparison of four different configuration for GOS synthesis with free enzyme in a discontinuous batch-reactor and with immobilized enzyme in 1 mL-, 8 mL- and 80 mL-PTFRs with semi-continuous, continuous and recirculation configuration ($ILC = 100 \text{ g L}^{-1}$).

The comparison of all four configurations with regard to maximum GOS yield revealed a significant increase (Figure 5b). In the discontinuous batch reactor, the highest GOS yield with 23% was achieved after 80 min. Furthermore, with the immobilized PTFRs in semi-continuous configuration (flow: 1 mL min^{-1} for the 1 mL-PTFR, 10 mL min^{-1} for 8- and 80 mL-PTFR) a yield up to 37% was achieved, although the residence time is only about 10 min. This certainly corresponds to the number of cycles, which was 38 for the 1 mL-monolith, 28 for the 8 mL- and 10 cycles for the 80 mL-PTFR. The enhanced yield can therefore only be achieved with an increased E/S ratio or STY in the smaller reactor space with its higher enzyme density in the immobilized PTFRs compared to the free enzyme in batch reactors. The larger the PTFR, the more units of enzyme (absolute) (Tables 1 and 2) are available for the GOS synthesis, and the fewer cycles are required to reach the maximum. The flow rates for continuous process management of the PTFRs to achieve maximum yields were 1 mL min^{-1} for the 1 mL-PTFR and 10 mL min^{-1} for the 8- and 80 mL-PTFR (Figure 5b). Here, the 80 mL-PTFR delivers by far the highest yield due to the larger available area with a higher total amount of immobilized enzyme. For the recirculation configuration (Figure 5b) the ratio between feed and recirculation flow was 1:10, with a flow through the monolith of 1 mL min^{-1} for the 1 mL-monolith and 10 mL min^{-1} for the 8- and 80 mL-PTFR. GOS synthesis with the recirculation configuration, i.e., a coupling of the semi-continuous and continuous processes was able to achieve a significant increase for

the 1 mL- and 8 mL-PTFR compared to the continuous system. In contrast, the 80 mL-PTFR with recirculation is an exception as no increase in GOS yield could be achieved with this scale. Two possible explanations seem reasonable for this observation. Firstly, the feed concentration of lactose is reduced by back-mixing with products (GOS, glucose, galactose), decreasing the reaction rate and conversion, respectively. Another reason could be the beginning degradation of GOS, which might encourage due to the PTFR-length or the higher number of enzymes.

2.3. Long-Term Stability of Immobilized Enzyme

Most important requirement for continuous operation by means of immobilized enzymes is the enzyme's long-term stability and activity, respectively. The decrease in the stability of the enzyme activity of the immobilized enzymes on the 8 mL- and 80 mL-PTFR was investigated in the semi-continuous mode regarding the lactose conversion in $\mu\text{mol per min (U)}$ and is shown in Figure 6 as the relative activity in %.

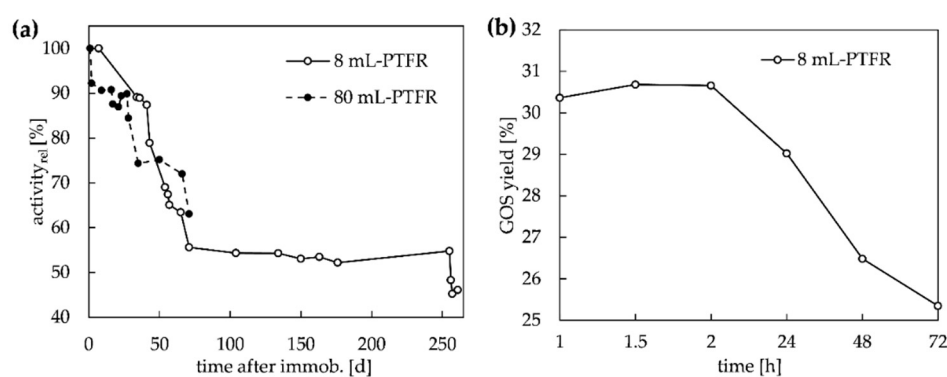


Figure 6. (a) relative enzyme activity of immobilized β -gal in 8 mL-PTFR (flow = 10 mL min^{-1}) and 80 mL-PTFR (flow = 20 mL min^{-1}) with semi-continuous configuration and (b) GOS yield of the continuous configuration with recirculation for the 8 mL-PTFR over 72 h ($p_1 = 0.5 \text{ mL min}^{-1}$, $p_2 = 9.5 \text{ mL min}^{-1}$).

The initial lactose conversion of each experiment was studied at flow rates of 10 mL min^{-1} for the 8 mL-PTFR and 20 mL min^{-1} for the 80 mL-PTFR (Figure 6a). The 8 mL-PTFR revealed a residual activity of 46% after 261 days (9 months) of intensive use including storage at 7°C (in $0.1 \text{ M Ka-Na-phosphate}$ buffer with 0.02% sodium azide). The enzyme on the 80 mL-PTFR still had a relative activity of 63% after 71 days. In Figure 6a, it can be seen that the course of the decrease in enzyme activity is very similar in both immobilized PTFRs. Thus, the use of CIM[®] monolithic PTFRs as immobilization support proves to be very suitable in terms of maintaining enzyme activity. High stability of the CIM[®] materials has also been reported in the literature, with an immobilized endodextranase remaining more than 78% active [37] and an immobilized ribonuclease remaining 77% active on epoxy monoliths after 28 days of storage. [25]. The immobilization of β -gal from *B. circulans* on Eupergit[®] beads was considered for longer periods and led to an enzyme half-time at a lactose concentration of 380 g L^{-1} of 90 days [17], which is in the same range as we observed for the 8 mL-PTFR. Whereas the enzyme stability on agarose beads was reported only for the actual time of use, remaining almost 100% stability over 4.7 h (14 cycles a 20 min) was obtained [39]. The decrease in GOS yield within a 3-day test in continuous configuration with recirculation (Figure 2d) is shown in Figure 6b. The permanent use of the enzyme leads to a decrease in the GOS yield of only 6% after 72 h.

2.4. Model-Based Studies

To evaluate the potential of the pore-through-flow membrane reactor, first simulation studies were carried out for a broad range of operating conditions. Estimated kinetic parameters from Table 2 (K_M , V_{max}) were implemented for modelling concentration profiles. The

reactor models for the reactor configurations studied are introduced in Section 3.5.4/ Table 4. Selected simulation studies are shown in Figure 7 using the example of semi-continuous operation of the disk-PTFR.

Table 4. Experimental and model-based characterization of the monolithic reactor.

Configuration	Mass Balance	IC/BC ¹
discontinuous batch	$\frac{dc_i}{dt} = \sum_{j=1}^M v_{ij} \cdot r_j$ (1)	$c_i = (t = 0) = c_i^0$
semi-continuous vessel:	$\frac{dc_i}{dt} = (c_i^0 - c_i) \frac{\dot{V}}{V}$ (2)	$c_i = (t = 0) = c_i^0$
coupled with the monolith:	$\frac{dc_i}{dz} = \frac{\varepsilon}{\tau} \frac{A}{V} \sum_{j=1}^M v_{ij} \cdot r_j$ (3)	$c_i = (z = 0) = c_i^0$
continuous vessel:	$\frac{dc_i}{dt} = 0$ (4)	
as tank for monolith:	$\frac{dc_i}{dz} = \frac{\varepsilon}{\tau} \frac{A}{V} \sum_{j=1}^M v_{ij} \cdot r_j$ (5)	$\dot{n}_{i,tot}^0 = \dot{n}_i^0 + \dot{n}_{i,rec}^0$

¹ IC = initial conditions, BC = boundary conditions.

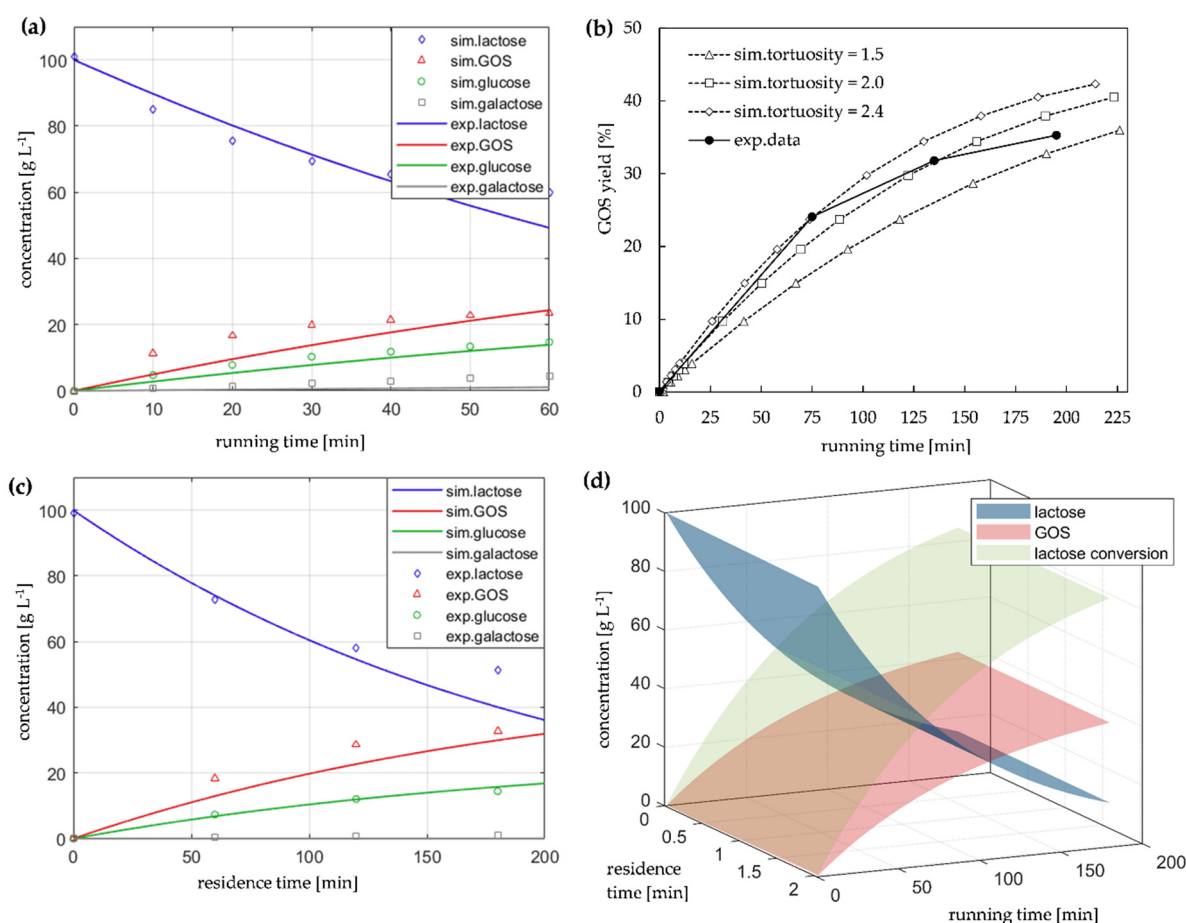


Figure 7. Modeling the GOS synthesis process with immobilized enzyme reactor: (a) reference system: concentration profiles of the discontinuous batch-reactor with free enzyme; (b) evaluation of tortuosity: GOS yield obtained with immobilized enzyme; (c) simulated and experimental data for immobilized enzyme; (d) 3D-plot of simulated data for the immobilized enzyme; (b–d) semi-continuous configuration with immobilized β -gal on disk-PTFR, flow = 0.1 mL min⁻¹.

Figure 7a shows the concentration profiles of the reference batch system with free enzyme and Figure 7c of the immobilized enzyme on PTFR, based on estimated kinetic data derived for the classical Michaelis-Menten approach. It becomes clear that corresponding

experimental data can be described by the reactor model applied. However, it also shows that the kinetic approach has limited applicability for a complex reaction network, such as GOS synthesis, and is certainly open for extension. The far more significant focus of the studies is on reactor/monolith modelling of the different modes of operation with the immobilized enzyme (Table 4). In this context, tortuosity of the monolithic structure plays a crucial role, as it is an important parameter influencing the transport processes in porous media. It describes the “geometry” of the transport pathways, where a tortuosity of 1 corresponds to a linear flow through the pores. The tortuosity for disk-PTFR was estimated with a value of 2, which offered the highest goodness of fit for the model-based description of GOS yield in Figure 7. Based on the models applied, influencing parameters can be analyzed for GOS synthesis as well as suitable experiments selected. Therefore, in Figure 7d lactose and GOS concentration as well as lactose conversion in a broad range of operating conditions (experimental running time, residence time/flow rate) are illustrated. The simulation results can subsequently be used to optimize process parameters and reactor configurations and are of importance for the evaluation of further scale-up strategies.

3. Materials and Methods

3.1. Chemicals and Enzymes

For GOS synthesis, determination of enzyme activity as well as for carbohydrate analysis the following chemicals were utilized from Carl Roth (Karlsruhe, Germany): lactose monohydrate, potassium di-hydrogen phosphate (KH_2PO_4), di-sodium hydrogen phosphate dihydrate ($\text{Na}_2\text{HPO}_4 \cdot 2\text{H}_2\text{O}$), sodium di-hydrogen phosphate dihydrate ($\text{NaH}_2\text{PO}_4 \cdot 2\text{H}_2\text{O}$), ethanoldiamine, sodium azide, sodium chloride (NaCl), solution for calorimetric protein determination (Roti[®]Quant Universal), albumin fraction V. A commercial β -gal from *B. circulans* was used. GOS, certified DOMO[®] Vivinal[®] syrup, with 44.25% galacto-oligosaccharides as standard for HPLC analysis was kindly provided by Friesland Campina (Amersfoort, The Netherlands).

3.2. Analysis of Carbohydrates

Carbohydrate contents before and during the reaction process were analyzed with HPLC (Chromaster[®] HPLC system, VWR, Darmstadt, Germany). The column Vertex Plus Eurokat Na, 10 μm , 300 \times 8 mm ID with a 30 \times 8 mm ID precolumn (Knauer GmbH, Berlin, Germany) was used with a flow rate of 0.25 mL min^{-1} , ultrapure water with 0.02% sodium azide (*w/v*) as eluent and a sample injection volume of 10 μL . The column was kept at a temperature of 85 $^\circ\text{C}$ and detection was carried out at 40 $^\circ\text{C}$ with a refractive index detector. The synthesized GOS yield was calculated in relation to initial lactose concentration (ILC) [10].

3.3. Monolithic Pore-Through Flow Reactor and Enzyme Immobilization

CIM[®] carboxyimidazole (CDI) activated monoliths from BIA Separations with a pore size of 1.3 μm were used as supports for β -gal immobilization and applied as pore-through-flow reactors (PTFR). Monoliths in the shape of a disk with a total volume of 0.34 mL were inserted in special housings. Experiments on upscaling were carried out with the 1 mL-, 8 mL- and 80 mL monolithic PTFRs in a cylindrical shape (Figure 8). The immobilization procedure was performed according to the application protocol of BIA Separations [35]. A 0.5 M Na-phosphate buffer, pH 8 was used as immobilization buffer. After cycling the ligand solution (9 mg mL^{-1} β -gal in immobilization buffer) for three hours, the monoliths were sealed and stored for 64 h at 7 $^\circ\text{C}$. Thereafter, deactivation of residual CDI groups was performed with 1.8 M ethanolamine in immobilization buffer with a final pH of 9.

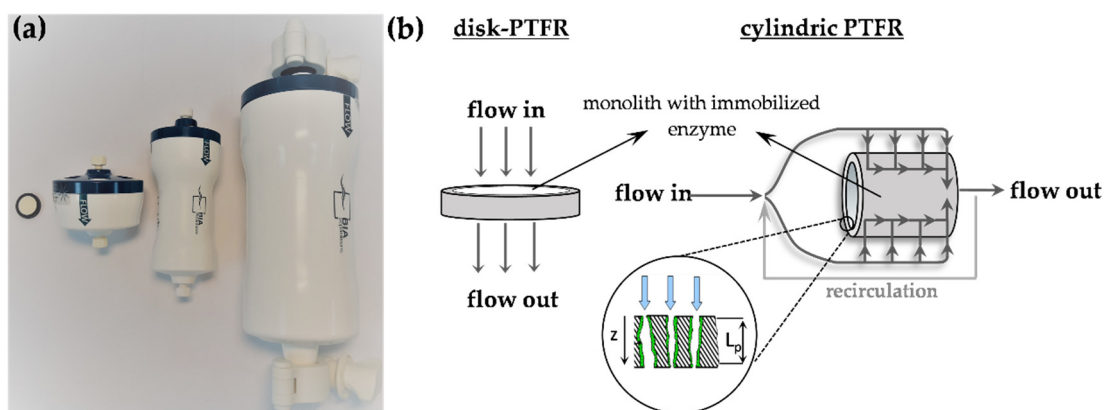


Figure 8. Design of monolithic PTFR: (a) disk-PTFR ($V = 0.34$ mL) and cylindrical PTFRs with a total volume of 1, 8 and 80 mL (from left to right); (b) schematic representation of the design and the flow regime in the PTFRs (L_p = pore length, z = running coordinate).

All steps were carried out at a flow rate of 0.5 mL min^{-1} for the disk-PTFR, 1 mL min^{-1} for the 1 mL- and 8 mL-PTFR and 10 mL min^{-1} for the 80 mL-PTFR, realized with a HPLC pump at room temperature. The working buffer, used for equilibration of the loaded monoliths and for GOS synthesis was 0.1 M Na-K-phosphate, pH 7.5. The loaded monoliths were stored in working buffer with 0.02% sodium azide (w/v) at 7°C .

3.4. Protein Analysis

The protein content of the β -gal powder and the amount of the immobilized enzyme (before and after immobilization) were determined by a Biuret based reaction [41] using Roti[®]Quant Universal and albumin standard, following the quantitation protocol provided by the reagent manufacturer. The absorbance was measured at 506 nm using a UV-Vis spectrophotometer.

3.5. Experimental and Model-Based Reactor Configurations for the Production of GOS by β -Galactosidase

3.5.1. GOS Synthesis with Free Enzyme

9.2 mg protein was added to 40 mL of a 100 g L^{-1} (w/v) lactose solution in 0.1 M Na-K-phosphate buffer, pH 7.5 at 35°C in a beaker with stirrer (Figure 2a). The reaction was carried out for a total of 24 h. Samples for HPLC analysis were taken at several time intervals. The inactivation of the enzymes was obtained through heating the samples at 90°C for at least five minutes [42].

3.5.2. GOS Synthesis in Enzyme Immobilized PTFRs

The enzyme loaded PTFRs were previously equilibrated with working buffer at 35°C . Subsequently, for the semi-continuous configuration (Figure 2b), a 100 g L^{-1} lactose solution in 0.1 M Na-K-phosphate buffer, pH 7.5 is initially flushed through the monolith and capillaries to discard the pure buffer solution from the system before closing the reactor system according to Figure 2b. For each monolithic scale, an appropriate total liquid volume of substrate solution was set in the system and kept constant during the studies at varying operating conditions. In all, $100 \mu\text{L}$ samples for HPLC analysis were taken at certain time intervals.

For the synthesis with the continuous configuration (Figure 2c) the immobilization system including the PTFR was completely purged with feed solution before taking samples with volumes of 1.5 mL at flow rates of $0.1/0.5/1.0/1.5 \text{ mL min}^{-1}$. All tests for the continuous system were carried out in duplicate. The configuration with recirculation (Figure 2d) was studied using the monolithic scales of 1 mL, 8 mL and 80 mL-PTFRs. Pump 2 partially recirculates the output of the PTFR into the front of the PTFR at defined flow

rate ratios between both pumps. The total flow rate through the PTFR results from the sum of feed and recirculation flow rates. The storage of the monolithic material between the attempts was carried out in 0.1 M Na-K-phosphate buffer with 0.02% sodium azide, pH 7.5.

3.5.3. Determination of Kinetic Parameters and Enzyme Activity

The calculation of the kinetic parameters as well as activities is based on the retention time, defined as the average residence time \bar{t} between enzyme and substrate.

For the batch modus, the residence time is equal to experimental runtime. In case of the immobilized enzyme, it is calculated according to Equation (6), wherein V_{tot} is the total volume of the PTFR, A_M is the membrane surface, L_p the pore length (Figure 8), τ is the tortuosity, w the velocity, \dot{V} the flow rate through the PTFR and ε is the estimated porosity of 0.3. Porosity was investigated using retention time analysis by pulse experiments with lactose injections onto the monoliths integrated into an HPLC system.

$$\bar{t} = \frac{V_{tot} \cdot \varepsilon}{\dot{V}} = \frac{A_M \cdot L_p \cdot \varepsilon}{\dot{V}} = \frac{L_p \cdot \varepsilon}{w \cdot \tau} \quad (6)$$

The calculation refers to one cycle, defined as the time required to circulate the whole volume of substrate solution through the monolith once in the semi-continuous system, or for a single pass through the monolithic module in the case of the continuous configuration.

Kinetic parameters were experimentally derived with the semi-continuous system and initial lactose concentrations of 50/100/150/200/220 g L⁻¹. In reference to the liquid volumes of the PTFRs (Table 1), maximum velocity (V_{max}) in mM lactose per min residence time and dissociation constants (K_M) in mM were determined by application of the Michaelis-Menten approach (Equation (2)) and Lineweaver-Burk linearization.

$$-\frac{dc_{lac}}{dt} = \frac{v_{max} \cdot c_{lac}}{K_M + c_{lac}} \quad (7)$$

Specific activity in units (U) per min residence time, was determined immediately after immobilization was accomplished with the semi-continuous configuration setup, shown in Figure 2b, and measurements were continued up to 250 days for the consideration of long-term stability. Therein, one unit is defined as the amount of enzyme that catalyzes the conversion of one μ mol of lactose per min in the liquid reactor volume and were calculated from the V_{max} .

The turnover number (k_{cat}), defined as the number of substrate molecules converted per single enzyme active site, per residence time and liquid reactor volume is calculated from V_{max} and the amount of substance of β -gal (248 kDa, from enzyme database BRENDA). The space-time-yield (STY) was determined as the maximum GOS yield per liquid reactor volume and with respect to the total experimental time. All calculations are based on the data obtained within a few days after finishing the immobilization and with the semi-continuous configuration at a flow rate of 0.5 mL min⁻¹ for disk- and 1 mL-PTFR, 10 mL min⁻¹ for the 8 mL-PTFR and 20 mL min⁻¹ for the 80 mL-PTFR.

3.5.4. Modeling of PTFR Configurations

All reactor configurations introduced in Figure 2 were modelled to perform simulation studies in a broad range of operation parameters in order to identify optimal operation conditions and for scale up. The discontinuous stirred batch reactor is assumed to be ideally mixed and the PTFR as plug flow reactor convective dominated [43–47]. Isothermal operation is assumed. For the mass balances and initial (IC)/boundary conditions (BC), the conditions in Table 4 apply.

4. Conclusions

Studies on β -gal from *B. circulans* immobilized on CDI activated monolithic PTFRs for GOS synthesis were conducted and compared to a free enzyme system. In addition, the

research also focused on the scale-up of the carrier-bound enzyme system with monolith sizes ranging from 0.34 mL up to 80 mL, which are used in their operational management as pore-through-flow reactors. The scale-up of the PTFRs revealed a high degree of correspondence between the carrier sizes with regard to the kinetic parameters, the enzyme loading and/or activity and the maximum GOS yield. In this context, a successful 3-stage scale-up of the enzyme immobilized carrier up to 80 mL of total carrier size was shown. Three different reactor operation configurations were examined and evaluated: semi-continuous, continuous and continuous with ratio-controlled recirculation. The results regarding the influence of various parameters (flow, residence times, flow ratios) on the GOS yield were shown to be directly transferable to larger sizes of the monolithic support. In addition, for all PTFR systems a significant increase in GOS yield of up to 60% compared to the single-used free enzyme in batch system could be obtained.

The long-time stability of the immobilized enzyme on the monolithic PTFRs could be proven, which is an essential requirement for the development of a continuous production process with immobilized enzyme systems. After 9 months of intensive use, a residual activity of 46% was observed. Furthermore, the reactor configurations were modelled, and simulation studies were performed. The applied reactor models could be validated based on experimental data from batch and disk-PTFR allowing a good description of the GOS formation process and providing a tool for further scale-up strategies. As perspective, studies with more complex kinetic modelling approaches in combination with adjusted reactor configuration strategies for monolith sizes ≥ 80 mL for industrial production would be conceivable.

Author Contributions: Conceptualization, I.P., I.M. and C.H.; methodology, I.P., I.M. and C.H.; software, I.P. and I.M.; validation, I.P. and I.M.; formal analysis, I.P.; investigation, I.P.; resources, C.H.; data curation, I.P.; writing—original draft preparation, I.P. and I.M.; writing—review and editing, C.H.; visualization, I.P.; supervision, C.H.; project administration, C.H.; funding acquisition, C.H. All authors have read and agreed to the published version of the manuscript.

Funding: This research was funded by the German Federal Ministry of Education and research (BMBF) within the framework of Research at Universities of Applied Sciences 2018 (project number: 13FH574IX6).

Acknowledgments: The authors gratefully acknowledge the funding by the German Federal Ministry of Education and like to appreciate the project partner BIA Separations for the providing monolithic hardware, visual material and technical support. Vivinal GOS-syrup was kindly provided by Friesland Campina (Amersfoort, The Netherlands).

Conflicts of Interest: The authors declare that they have no known competing financial interests or personal relationships that could have appeared to influence the work reported in this paper.

References

1. Gänzle, M.G.; Haase, G.; Jelen, P. Lactose: Crystallization, hydrolysis and value-added derivatives. *Int. Dairy J.* **2008**, *18*, 685–694. [[CrossRef](#)]
2. Gibson, G.R.; Hutkins, R.; Sanders, M.E.; Prescott, S.L.; Reimer, R.A.; Salminen, S.J.; Scott, K.; Stanton, C.; Swanson, K.S.; Cani, P.D.; et al. Expert consensus document: The International Scientific Association for Probiotics and Prebiotics (ISAPP) consensus statement on the definition and scope of prebiotics. *Nat. Rev. Gastroenterol. Hepatol.* **2017**, *14*, 491–502. [[CrossRef](#)] [[PubMed](#)]
3. Tanaka, R.; Takayama, H.; Morotomi, M.; Kuroshima, T.; Ueyama, S.; Matsumoto, K.; Kuroda, A.; Mutai, M. Effects of administration of TOS and *Bifidobacterium breve* 4006 on the human fecal flora. *Bifidobact. Microflora* **1983**, *2*, 17–24. [[CrossRef](#)]
4. Sangwan, V.; Tomar, S.K.; Singh, R.R.; Singh, A.K.; Ali, B. Galactooligosaccharides: Novel components of designer foods. *J. Food Sci.* **2011**, *76*, R103–R111. [[CrossRef](#)]
5. Kunz, C.; Rudloff, S.; Baier, W.; Klein, N.; Strobel, S. OLIGOSACCHARIDES IN HUMAN MILK: Structural, Functional, and Metabolic Aspects. *Annu. Rev. Nutr.* **2000**, *20*, 699–722. [[CrossRef](#)] [[PubMed](#)]
6. Urashima, T.; Taufik, E. Oligosaccharides in Milk: Their Benefits and Future Utilization. *Media Peternak.* **2010**, *33*, 189–197. [[CrossRef](#)]
7. Gosling, A.; Stevens, G.W.; Barber, A.R.; Kentish, S.E.; Gras, S.L. Recent advances refining galactooligosaccharide production from lactose. *Food Chem.* **2010**, *121*, 307–318. [[CrossRef](#)]

8. Torres, D.P.M.; Gonçalves, M.d.P.F.; Teixeira, J.A.; Rodrigues, L.R. Galacto-oligosaccharides: Production, properties, applications, and significance as prebiotics. *Compr. Rev. Food Sci. Food Saf.* **2010**, *9*, 438–454. [[CrossRef](#)]
9. Fischer, C.; Kleinschmidt, T. Synthesis of Galactooligosaccharides in Milk and Whey: A Review. *Compr. Rev. Food Sci. Food Saf.* **2018**, *17*, 678–697. [[CrossRef](#)]
10. Mueller, I.; Kiedorf, G.; Runne, E.; Seidel-Morgenstern, A.; Hamel, C. Synthesis, kinetic analysis and modelling of galacto-oligosaccharides formation. *Chem. Eng. Res. Des.* **2018**, *130*, 154–166. [[CrossRef](#)]
11. Cao, L. Introduction: Immobilized enzymes: Past, present and prospects. In *Carrier-Bound Immobilized Enzymes: Principles, Application and Design*; John Wiley & Sons: Hoboken, NJ, USA, 2005.
12. Ureta, M.M.; Martins, G.N.; Figueira, O.; Pires, P.F.; Castilho, P.C.; Gomez-Zavaglia, A. Recent advances in β -galactosidase and fructosyltransferase immobilization technology. *Crit. Rev. Food Sci. Nutr.* **2020**, *61*, 2659–2690. [[CrossRef](#)] [[PubMed](#)]
13. Sass, A.C.; Jördening, H.J. Immobilization of β -Galactosidase From *Aspergillus oryzae* on Electrospun Gelatin Nanofiber Mats for the Production of Galactooligosaccharides. *Appl. Biochem. Biotechnol.* **2020**, *191*, 1155–1170. [[CrossRef](#)] [[PubMed](#)]
14. Misson, M.; Jin, B.; Dai, S.; Zhang, H. Interfacial biocatalytic performance of nanofiber-supported β -galactosidase for production of galacto-oligosaccharides. *Catalysts* **2020**, *10*, 81. [[CrossRef](#)]
15. Huerta, L.M.; Vera, C.; Guerrero, C.; Wilson, L.; Illanes, A. Synthesis of galacto-oligosaccharides at very high lactose concentrations with immobilized β -galactosidases from *Aspergillus oryzae*. *Process Biochem.* **2011**, *46*, 245–252. [[CrossRef](#)]
16. Benjamins, E. Galacto-Oligosaccharide Synthesis Using Immobilized β -Galactosidase. Ph.D. Thesis, Rijksuniversiteit, University of Groningen, Groningen, The Netherlands, 2014.
17. Warmerdam, A.; Benjamins, E.; de Leeuw, T.F.; Broekhuis, T.A.; Boom, R.M.; Janssen, A.E.M. Galacto-oligosaccharide production with immobilized β -galactosidase in a packed-bed reactor vs. free β -galactosidase in a batch reactor. *Food Bioprod. Processing* **2014**, *92*, 383–392. [[CrossRef](#)]
18. Carević, M.; Čorović, M.; Mihailović, M.; Banjanac, K.; Milisavljević, A.; Veličković, D.; Bezbradica, D. Galacto-oligosaccharide synthesis using chemically modified β -galactosidase from *Aspergillus oryzae* immobilised onto macroporous amino resin. *Int. Dairy J.* **2016**, *54*, 50–57. [[CrossRef](#)]
19. Hackenhaar, C.R.; Spolidoro, L.S.; Flores, E.; Klein, M.P.; Hertz, P.F. Batch synthesis of galactooligosaccharides from co-products of milk processing using immobilized β -galactosidase from *Bacillus circulans*. *Biocatal. Agric. Biotechnol.* **2021**, *36*, 102136. [[CrossRef](#)]
20. Klein, M.P.; Fallavena, L.P.; Schöffner, J.; Ayub, M.; Rodrigues, R.C.; Ninow, J.L.; Hertz, P.F. High stability of immobilized β -d-galactosidase for lactose hydrolysis and galactooligosaccharides synthesis. *Carbohydr. Polym.* **2013**, *95*, 465–470. [[CrossRef](#)]
21. Urrutia, P.; Mateo, C.; Guisan, J.M.; Wilson, L.; Illanes, A. Immobilization of *Bacillus circulans* β -galactosidase and its application in the synthesis of galacto-oligosaccharides under repeated-batch operation. *Biochem. Eng. J.* **2013**, *77*, 41–48. [[CrossRef](#)]
22. Štrancar, A.; Barut, M.; Podgornik, A.; Koselj, P.; Schwinn, H.; Raspor, P.; Josić, D. Application of compact porous tubes for preparative isolation of clotting factor VIII from human plasma. *J. Chromatogr. A* **1997**, *760*, 117–123. [[CrossRef](#)]
23. Vodopivec, M.; Podgornik, A.; Berovič, M.; Štrancar, A. Characterization of CIM monoliths as enzyme reactors. *J. Chromatogr. B* **2003**, *795*, 105–113. [[CrossRef](#)]
24. Podgornik, A.; Štrancar, A. Convective Interaction Media[®] (CIM)—Short layer monolithic chromatographic stationary phases. In *Biotechnology Annual Review*; Elsevier: Amsterdam, The Netherlands, 2005.
25. Benčina, M.; Babič, J.; Podgornik, A. Preparation and characterisation of ribonuclease monolithic bioreactor. *J. Chromatogr. A* **2007**, *1144*, 135–142. [[CrossRef](#)] [[PubMed](#)]
26. Barut, M.; Podgornik, A.; Brne, P.; Štrancar, A. Convective Interaction Media short monolithic columns: Enabling chromatographic supports for the separation and purification of large biomolecules. *J. Sep. Sci.* **2005**, *28*, 1876–1892. [[CrossRef](#)]
27. Mao, Y.; Černigoj, U.; Zalokar, V.; Štrancar, A.; Kulozik, U. Production of β -Lactoglobulin hydrolysates by monolith based immobilized trypsin reactors. *Electrophoresis* **2017**, *38*, 2947–2956. [[CrossRef](#)] [[PubMed](#)]
28. Mao, Y.; Krischke, M.; Hengst, C.; Kulozik, U. Comparison of the influence of pH on the selectivity of free and immobilized trypsin for β -lactoglobulin hydrolysis. *Food Chem.* **2018**, *253*, 194–202. [[CrossRef](#)] [[PubMed](#)]
29. Mao, Y.; Krischke, M.; Hengst, C.; Kulozik, U. Influence of salts on hydrolysis of β -lactoglobulin by free and immobilised trypsin. *Int. Dairy J.* **2019**, *93*, 106–115. [[CrossRef](#)]
30. Nicoli, R.; Gaud, N.; Stella, C.; Rudaz, S.; Veuthey, J.L. Trypsin immobilization on three monolithic disks for on-line protein digestion. *J. Pharm. Biomed. Anal.* **2008**, *48*, 398–407. [[CrossRef](#)] [[PubMed](#)]
31. Naldi, M. Towards automation in protein digestion: Development of a monolithic trypsin immobilized reactor for highly efficient on-line digestion and analysis. *Talanta* **2017**, *167*, 143–157. [[CrossRef](#)]
32. Sproß, J.; Sinz, A. A Capillary monolithic trypsin reactor for efficient protein digestion in online and offline coupling to ESI and MALDI mass spectrometry. *Anal. Chem.* **2010**, *82*, 1434–1443. [[CrossRef](#)]
33. Benčina, K.; Podgornik, A.; Štrancar, A.; Benčina, M. Enzyme immobilization on epoxy- and 1,1'-carbonyldiimidazole-activated methacrylate-based monoliths. *J. Sep. Sci.* **2004**, *27*, 811–818. [[CrossRef](#)]
34. Pottratz, I.; Schmidt, C.; Müller, I.; Hamel, C. Immobilization of β -Galactosidase on Monolithic Discs for the Production of Prebiotics Galacto-oligosaccharides. *Chem. Ing. Tech.* **2021**, *93*, 838–843. [[CrossRef](#)]
35. BIA Separation. Available online: <https://www.biaseparations.com/en/products/monolithic-columns/products-for-immobilization-screening> (accessed on 20 July 2020).

36. Guerrero, C.; Aburto, C.; Suárez, S.; Vera, C.; Illanes, A. Effect of the type of immobilization of β -galactosidase on the yield and selectivity of synthesis of transgalactosylated oligosaccharides. *Biocatal. Agric. Biotechnol.* **2018**, *16*, 353–363. [[CrossRef](#)]
37. Bertrand, E.; Pierre, G.; Delattre, C.; Gardarin, C.; Bridiau, N.; Maugard, T.; Štrancar, A.; Michaud, P. Dextranase immobilization on epoxy CIM[®] disk for the production of isomaltooligosaccharides from dextran. *Carbohydr. Polym.* **2014**, *111*, 707–713. [[CrossRef](#)] [[PubMed](#)]
38. Abou-Rebyeh, H.; Körber, F.; Schubert-Rehberg, K.; Reusch, J.; Josić, D. Carrier membrane as a stationary phase for affinity chromatography and kinetic studies of membrane-bound enzymes. *J. Chromatogr. B Biomed. Sci. Appl.* **1991**, *566*, 341–350. [[CrossRef](#)]
39. Rodriguez-Colinas, B.; Fernandez-Arrojo, L.; Santos-Moriano, P.; Ballesteros, A.O.; Plou, F.J. Continuous packed bed reactor with immobilized β -Galactosidase for production of galactooligosaccharides (GOS). *Catalysts* **2016**, *6*, 189. [[CrossRef](#)]
40. Tennikova, T.B.; Svec, F.; Belenkii, B.G. High-Performance Membrane Chromatography. A Novel Method of Protein Separation. *J. Liq. Chromatogr.* **1990**, *13*, 63–70. [[CrossRef](#)]
41. Smith, P.K.; Krohn, R.I.; Hermanson, G.T.; Mallia, A.K.; Gartner, F.H.; Provenzano, M.D.; Fujimoto, E.K.; Goetze, N.M.; Olson, B.J.; Klenk, D.C. Measurement of protein using bicinchoninic acid. *Anal. Biochem.* **1985**, *150*, 76–85. [[CrossRef](#)]
42. Mueller, I.; Kiedorf, G.; Runne, E.; Pottratz, I.; Seidel-Morgenstern, A.; Hamel, C. Process Control and Yield Enhancement of the Galacto-Oligosaccharide Formation. *Chem. Ing. Tech.* **2018**, *90*, 725–730. [[CrossRef](#)]
43. Schmidt, A.; Haidar, R.; Schomäcker, R. Selectivity of partial hydrogenation reactions performed in a pore-through-flow catalytic membrane reactor. *Catal. Today* **2005**, *104*, 305–312. [[CrossRef](#)]
44. Caro, J. Contactor-type catalytic membrane reactor. In *Encyclopedia of Membranes*; Drioli, E., Giorno, L., Eds.; Springer: Berlin, Heidelberg, Germany, 2016; pp. 445–446, ISBN 978-3-662-44324-8.
45. Seidel-Morgenstern, A. *Membrane Reactors: Distributing Reactants to Improve Selectivity and Yield*; Wiley-VCH: Hoboken, NJ, USA, 2010; ISBN 9783527320394.
46. Hertwig, K.; Martens, L.; Hamel, C. *Chemische Verfahrenstechnik*; De Gruyter: Oldenburg, Germany, 2018; ISBN 978-3-11-0500099-8.
47. Dittmeyer, R.; Pfeifer, P.; Brandner, J.J.; Kraut, M. *Micro Process Engineering—Explained*; De Gruyter: Oldenburg, Germany, 2021; ISBN 978-3110265385.